

The ridge in proton-proton collisions at the LHC

Adrian Dumitru,^{1,2} Kevin Dusling,³ François Gelis,⁴
Jamal Jalilian-Marian,² Tuomas Lappi,^{5,6} and Raju Venugopalan³

¹*RIKEN BNL Research Center, Brookhaven National Laboratory, Upton, NY-11973, USA*

²*Department of Natural Sciences, Baruch College, CUNY,*

17 Lexington Avenue, New York, NY 10010, USA

³*Physics Department, Brookhaven National Laboratory, Upton, NY-11973, USA*

⁴*Institut de Physique Théorique (URA 2306 du CNRS),*

CEA/DSM/Saclay, 91191, Gif-sur-Yvette Cedex, France

⁵*Department of Physics, P.O. Box 35, 40014 University of Jyväskylä, Finland*

⁶*Helsinki Institute of Physics, P.O. Box 64, 00014 University of Helsinki, Finland*

We show that the key features of the CMS result on the ridge correlation seen for high multiplicity events in $\sqrt{s} = 7$ TeV proton-proton collisions at the LHC can be understood in the Color Glass Condensate framework of high energy QCD. The same formalism underlies the explanation of the ridge events seen in A+A collisions at RHIC, albeit it is likely that flow effects may enhance the magnitude of the signal in the latter.

I. INTRODUCTION

A very recent preprint [1] from the CMS collaboration at the LHC reports the observation of a ridge-like structure of correlated charged particle pairs with momenta in the range $p_{\perp}, q_{\perp} \sim 1\text{--}3$ GeV in high multiplicity (with $N \geq 110$) events in proton-proton collisions at $\sqrt{s} = 7$ TeV. This ridge is a feature on the “near side” of the two particle correlation, around $\Delta\phi \approx 0$ azimuthal separation between the two particles. It extends at least up to $\Delta\eta \approx 4.8$, the limit of acceptance of the detector components used in the analysis. The ridge is seen only in the moderate p_{\perp}, q_{\perp} range and systematically vanishes for $p_{\perp}, q_{\perp} \lesssim 1$ GeV and $p_{\perp}, q_{\perp} \gtrsim 3$ GeV. A plot summarizing this structure in the CMS data is shown in fig. 1.

A similar ridge-like structure was previously seen in nucleus-nucleus collisions at RHIC [2–7]. The ridge was seen in high multiplicity (central) events in Cu+Cu collisions at $\sqrt{s} = 62.4$ GeV and in Au+Au collisions at $\sqrt{s} = 200$ GeV. The STAR detector observed this correlation for both p_{\perp} -triggered [2, 5] and untriggered [3] pair correlations in the whole STAR TPC acceptance of $\Delta\eta \leq 2$. The PHOBOS experiment [6] observed the p_{\perp} -triggered correlation at much larger rapidity separations, initially up to $\Delta\eta \sim 4$, extended more recently [7] to $\Delta\eta \sim 5$. The long range correlation structure disappears for lower multiplicity peripheral events in nucleus-nucleus collisions and are also absent in deuteron-gold and proton-proton “control” experiments at the same energies. The STAR and PHOBOS correlation results are shown in fig. 2.

Why is the ridge interesting? One can show from a simple argument based on causality [8] that if long range rapidity correlations between particles exist, the correla-

tion must be formed at proper times earlier than¹

$$\tau_{\text{init.}} = \tau_{\text{f.o.}} \exp\left(-\frac{1}{2}\Delta y\right), \quad (1)$$

where $\tau_{\text{f.o.}}$ is the freeze-out time of the particles. This causality argument is illustrated in fig. 3. If we assume this freeze-out time to be of the order of a few fermis, a rapidity correlation of $\Delta\eta \sim 5$ units suggests that these correlations must be formed nearly instantaneously after the collision or must preexist in the incoming projectiles. They are therefore very sensitive to the strong color fields present in the initial stage and their correlations.

In a recent paper [9] (see also [10, 11]), it was shown in detail how these long range correlations arise as a consequence of the saturation of gluons with momenta $k_{\perp} \leq Q_s$ in the nuclear wave functions *before* the collision. Here $Q_s > \Lambda_{\text{QCD}}$ is a semi-hard saturation scale [12, 13], which provides a measure of the range of color correlations in a *nucleon or nucleus*. This scale is large for *either high energies or large nuclei or both*, suggesting the presence of strong universal dynamical color correlations at distances smaller than the scale of confinement dynamics $1/\Lambda_{\text{QCD}}$ in QCD. Because Q_s is large, a quantitative understanding of the highly non-perturbative dynamics of saturated gluons in feasible in weak coupling, and is realized in the Color Glass Condensate (CGC) effective theory [14–16] of hadron and nuclear wavefunctions at high energies. The reference [9] provides a quantitative comparison with the PHOBOS data and makes predictions for similar correlations in A+A collisions at the LHC.

When two hadrons or nuclei collide at high energies, the CGC framework predicts that strong longitudinal chromo-electric and chromo-magnetic fields are produced

¹ This argument assumes that a produced particle’s momentum space rapidity is tightly correlated with its space-time rapidity.

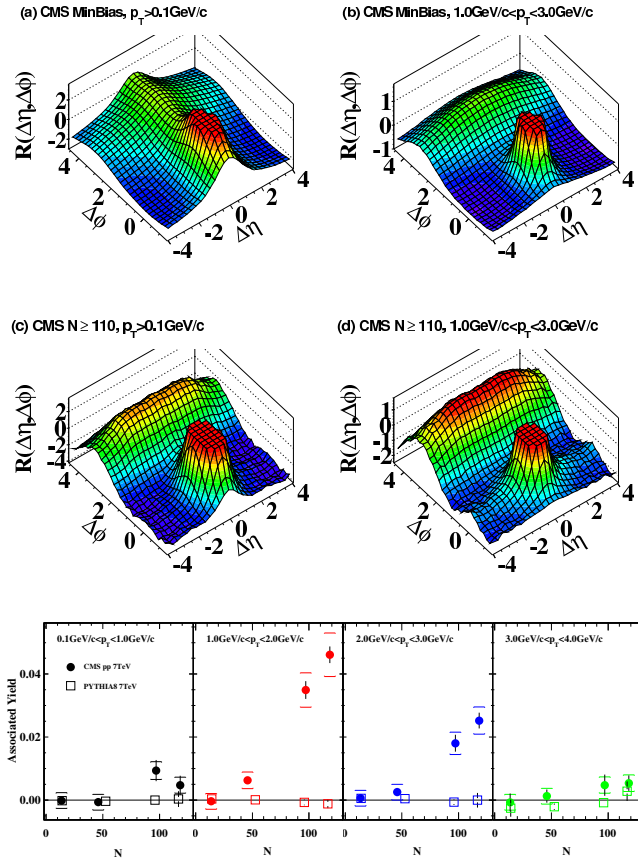


FIG. 1: Top: 3-D display of the two particle correlation R as a function of $\Delta\eta$ and $\Delta\phi$ for minimum bias and high multiplicity events in two different p_{\perp} windows. Bottom: The associated yield in different p_{\perp} windows as a function of the number of charged particle tracks. From ref. [1].

that are nearly boost-invariant [17, 18]; this form of matter has been called the Glasma [19]. We should emphasize here at the outset that the properties of the Glasma are not computed in an *ad hoc* model but follow from high energy factorization theorems which relate multi-particle dynamics in the Glasma to multi-parton correlations in saturated hadron/nuclear wavefunctions [11, 20, 21]. A key feature of the Glasma is that the transverse correlation length of these strong longitudinal chromo-electric and chromo-magnetic fields is $1/Q_s$. Two-particle [8, 22, 23] and three-particle [24] correlations were computed in this Glasma “flux tube” picture. We should note that the n -particle correlations can be shown to satisfy a negative binomial distribution [25]—providing a microscopic derivation of this widely used multiplicity distribution. These correlations are independent of $\Delta\eta$ up to quantum corrections that become important for $\Delta\eta \gtrsim 1/\alpha_s$. In heavy ion collisions the collimation in $\Delta\phi$ comes primarily from the subsequent radial flow of the correlated particles [26–31].

However, as discussed in more detail below, an intrinsic

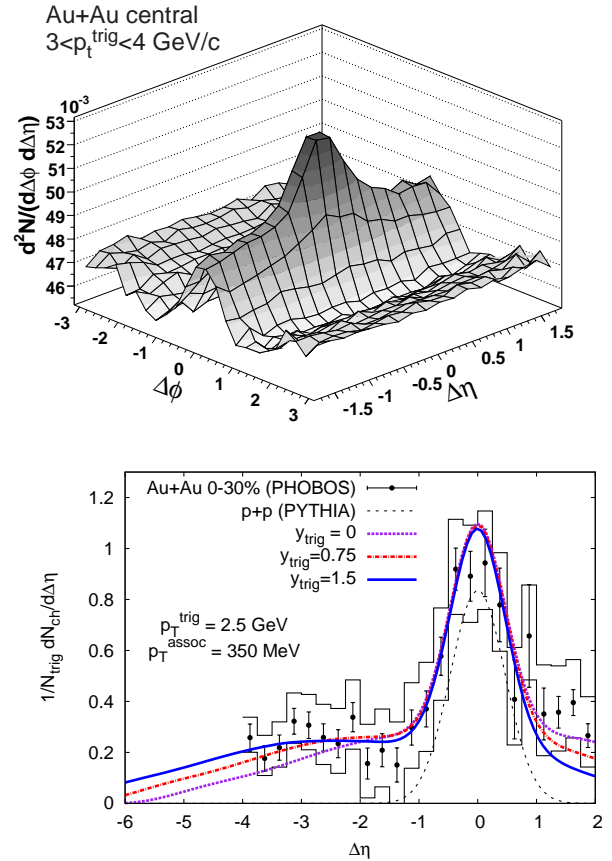


FIG. 2: Top: 3-D display of the two particle correlation (analogous to R in fig. 1) for p_{\perp} -triggered events from the STAR collaboration [5] (note that the away-side peak around $\Delta\phi = \pi$ seen in fig. 1 has been removed). Bottom: Two-particle correlation data from the PHOBOS collaboration [6] that reveals a long range component. The curves shown are obtained by adding our result (in eq. (3)) to the short range correlation from PYTHIA.

$\Delta\phi$ collimation is also present independently of the effects from flow in the later stages of the collision. It is very weak for the small Q_s values that are attained in p+p, d+A and peripheral A+A collisions at RHIC. At LHC energies, for the large multiplicity cuts performed by the CMS experiment (which select central impact parameters), the signal is stronger because Q_s is larger but not as strong as in central A+A collisions, because the effect of radial flow is smaller or absent. Indeed, “predictions” previous to the CMS announcement existed [32] but were not submitted for publication because it appeared inconceivable that such a small signal would be detected experimentally—this places the *tour de force* measurement by CMS in perspective!

We shall now show some of our results that exhibit the same qualitative features as the CMS results. More quantitative comparisons would require a more detailed understanding of the impact parameter dependence af-

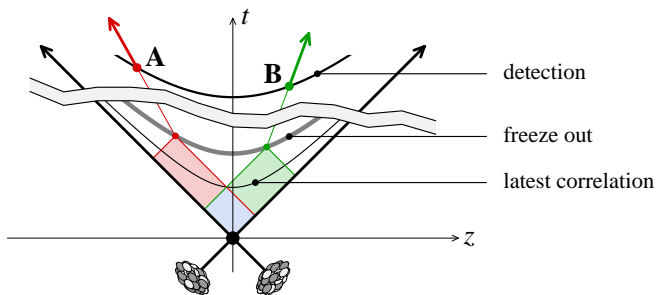


FIG. 3: This figure illustrates the argument from causality that long range correlations of particles (denoted A and B here) must occur at very early proper times. The doubly shaded region, corresponding to the intersection of the light cones of the two particles, is the space-time location where correlations can be formed.

fecting the normalization, experimental efficiency and acceptance effects and the contribution of radial flow. We hope to be able to make more detailed comparisons in the near future.

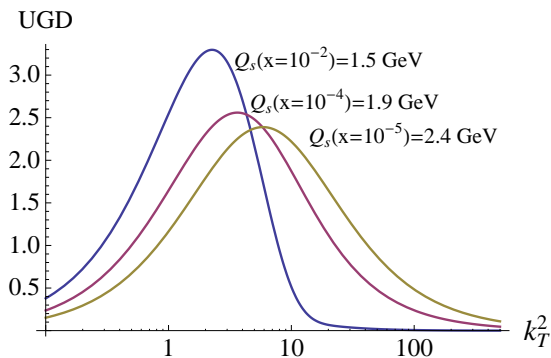


FIG. 4: The unintegrated gluon distribution as a function of transverse momentum squared for running coupling for three values of the momentum fraction x .

II. LONG RANGE TWO-PARTICLE CORRELATION

The strength of two-particle correlations is conveniently represented by the function

$$C_2(\mathbf{p}_\perp, y_p, \mathbf{q}_\perp, y_q) \equiv \frac{dN}{dy} \left[\frac{\frac{dN_2}{d^2\mathbf{p}_\perp d^2\mathbf{q}_\perp d^2\mathbf{q}_\perp}}{\frac{dN}{d^2\mathbf{p}_\perp d^2\mathbf{p}_\perp} \frac{dN}{d^2\mathbf{q}_\perp d^2\mathbf{q}_\perp}} - 1 \right], \quad (2)$$

The expression in eq. (2) corresponds (qualitatively) to the quantity $R(\Delta\phi, \Delta\eta)$ plotted in the CMS paper. Our result for the correlated two-particle distribution in

eq. (2) can be expressed as [9]

$$\begin{aligned} \frac{dN_2}{d^2\mathbf{p}_\perp dy_p d^2\mathbf{q}_\perp dy_q} &= \frac{\alpha_s^2}{16\pi^{10}} \frac{N_c^2 S_\perp}{(N_c^2 - 1)^3 \mathbf{p}_\perp^2 \mathbf{q}_\perp^2} \\ &\times \int d^2\mathbf{k}_\perp \left\{ \Phi_A^2(y_p, \mathbf{k}_\perp) \Phi_B(y_p, \mathbf{p}_\perp - \mathbf{k}_\perp) \right. \\ &\quad \times [\Phi_B(y_q, \mathbf{q}_\perp + \mathbf{k}_\perp) + \Phi_B(y_q, \mathbf{q}_\perp - \mathbf{k}_\perp)] \\ &\quad + \Phi_B^2(y_q, \mathbf{k}_\perp) \Phi_A(y_p, \mathbf{p}_\perp - \mathbf{k}_\perp) \\ &\quad \left. \times [\Phi_A(y_q, \mathbf{q}_\perp + \mathbf{k}_\perp) + \Phi_A(y_q, \mathbf{q}_\perp - \mathbf{k}_\perp)] \right\}. \end{aligned} \quad (3)$$

Here the Φ 's are *unintegrated gluon distributions* (UGD) per unit of transverse area in projectiles A and B and S_\perp is the transverse overlap area of the two hadrons. Equation 3 is based on the formalism developed in [10, 11] and is derived in ref. [9]. The single inclusive gluon spectrum can be expressed in the same notation as [33–35]

$$\begin{aligned} \frac{dN}{d^2\mathbf{p}_\perp dy_p} &= \frac{\alpha_s N_c S_\perp}{\pi^4 (N_c^2 - 1)} \frac{1}{\mathbf{p}_\perp^2} \\ &\times \int \frac{d^2\mathbf{k}_\perp}{(2\pi)^2} \Phi_A(y_p, \mathbf{k}_\perp) \Phi_B(y_p, \mathbf{p}_\perp - \mathbf{k}_\perp). \end{aligned} \quad (4)$$

The above expressions (eqs. 3 and 4) are valid to leading logarithmic accuracy in x and for momenta $p_\perp, q_\perp \gtrsim Q_s$.

The important ingredient in the above expressions is the unintegrated gluon density which is a universal quantity and can be constrained from fits to DIS on hadron [36] and nuclear targets [9]—these unintegrated gluon densities have been used to compute single inclusive and double inclusive distributions in d+Au collisions at RHIC [37]. The only difference between different targets are in the initial conditions determined at an initial x_0 —chosen to be $x_0 = 0.01$. The evolution of the UGD with rapidity is controlled by the Balitsky–Kovchegov (BK) equation [38, 39], which is a non-linear evolution equation describing both gluon emission and multiple scattering effects. We note that our unintegrated gluon distributions have recently been shown to be equivalent to those derived in the framework of transverse momentum dependent (TMD) parton distributions [40]. In fig. 4 we show the structure of this unintegrated gluon distribution and its evolution with rapidity for a running coupling. The running of the coupling slows the evolution significantly which is essential to describe DIS and hadron scattering data.

III. THE RIDGE IN PROTON PROTON COLLISIONS

In proton–proton collisions, unlike nucleus–nucleus collisions, it is not clear that there can be a sufficient amount of transverse flow to provide the collimation around $\Delta\phi \approx 0$ necessary to explain the ridge. Blast wave fits to proton single particle spectra at low p_\perp are suggestive of

non-vanishing radial flow, and this in principle could provide an additional collimation of the signal. We also note that in the highest multiplicity proton-proton events the charged particle multiplicity per unit rapidity is comparable to that found in semi-central Cu-Cu collisions. The possibility that additional collimation of the signal due to flow might be needed to reproduce the full strength of the measured correlation cannot be completely ruled out. However, the absence of a correlation signal for small transverse momenta in proton-proton collisions (contrary to the nucleus-nucleus case) suggests that hydrodynamical flow would not be the dominant contribution here.

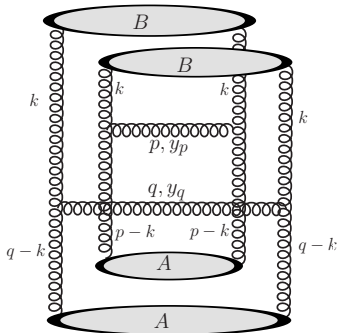


FIG. 5: A typical diagram which gives an angular collimation.

The main point of this paper is that there is an intrinsic angular correlation (in addition to the long range rapidity correlation) coming from the particle production process on transverse distance scales $1/Q_s$ much smaller than the proton size. One of the diagrams that gives a collimation for $\Delta\phi \approx 0$ is shown in fig. 5. There is only a single loop momentum \mathbf{k}_\perp in these two-particle production diagrams, as opposed to uncorrelated production. The transverse momenta flowing into the “blobs” for hadron A in this diagram are $|\mathbf{p}_\perp - \mathbf{k}_\perp|$ and $|\mathbf{q}_\perp - \mathbf{k}_\perp|$, respectively. If we combine this with the fact that the unintegrated distributions peak about Q_s (fig. 4) it follows that the *largest* contribution is obtained when both $|\mathbf{p}_\perp - \mathbf{k}_\perp| \sim Q_s$ and $|\mathbf{q}_\perp - \mathbf{k}_\perp| \sim Q_s$. These conditions are satisfied simultaneously, for one and the same \mathbf{k}_\perp , if \mathbf{p}_\perp and \mathbf{q}_\perp are parallel, leading to angular collimation. The scale of the angular dependence is $\mathcal{O}(1)$. Also, if parametrically p_\perp and q_\perp are much smaller or much greater than Q_s , the collimation disappears.

In contrast, in collinear factorization, at leading order both gluons are produced from the same ladder leading to collimation about $\Delta\phi \sim \pi$ (“dijet”). One may therefore expect that diagrams such as fig. 5 give a large contribution to $C(\mathbf{p}_\perp, y_p, \mathbf{q}_\perp, y_q)$ when $\Delta\phi \ll \pi$ and $|y_p - y_q| \gtrsim 1$ (see, also, discussion in ref. [10]).

Our results are summarized in figs. 6 and 7. In fig. 6 we show $C_2(\mathbf{p}_\perp, y_p, \mathbf{q}_\perp, y_q)$ for $p_\perp \approx q_\perp$ as a function of Q_0^2 , the saturation scale at the initial condition of the evolution $x = x_0$. A larger saturation scale corresponds to a more central collision and thus to a higher multiplicity. Thus our result shown in fig. 6 agrees with the CMS

observation of the ridge correlation becoming visible for higher multiplicity events. The exact relation between the value of Q_s and the observed multiplicity depends on the overlap area of the two protons and on the impact parameter dependence of the saturation scale (see e.g. [41, 42]). Establishing the normalization without additional free parameters would require going beyond the k_\perp -factorized expression (4) for the single inclusive spectrum [43]. However, in the appropriately normalized correlation (2) these factors cancel and our result does not depend strongly on the size of the overlap area. The result shown in fig. 6 is obtained by integrating over $\Delta\phi$ for $0 \leq \Delta\phi \leq \pi/2$. For a fixed p_\perp , we see that the correlation increases with centrality. The systematics is striking. For all centralities, the collimation is weak for low p_\perp . For $p_\perp > 1$ GeV, the correlation grows but at $p_\perp > 6$ GeV, the correlation decreases below the value at $p_\perp = 0.5$ GeV and is smaller for all higher p_\perp values. The reader should keep in mind that this result is for gluons. Fragmentation effects may approximately cancel in the C_2 ratio but the p_\perp of the hadrons is of course lower than that of the gluons. While this plot cannot be compared directly to fig. 1 (bottom) it shows a non trivial systematics very similar to it.

In fig. 7 (top) we plot the p_\perp dependence of C_2 . We see that the distribution is peaked approximately at the value of Q_s evolved to the rapidities of interest and that the correlations drop off sharply at large p_\perp . For low p_\perp , one has less theoretical control on how the distributions fall off but the trend is unmistakable. In fig. 7 (bottom), we show the rapidity dependence for fixed $p_\perp = q_\perp = 2$ GeV as a function of y_q , given two different y_p and two different values of Q_0 . For $y_p = 0$, we see that the distributions are symmetric around $y_q = 0$. This is not the case for $y_p = -3$, because QCD evolution (gluon radiation) between the projectiles to the produced gluons is asymmetric. The systematics could in principle be investigated to test our predictions in detail.

IV. SUMMARY

The physics of gluon saturation opens up a novel domain of many body QCD at high energies and may contain many surprises which provide deeper insight into the fundamental properties of strong interactions. One of these is the ridge in proton-proton collisions and it is likely that many more will be revealed at the LHC. The properties of saturated gluons, in particular the evolution of multi-parton correlations with energy, can be computed in the Color Glass Condensate effective field theory. High energy factorization theorems allow us to relate these multi-parton correlations in the hadron and nuclear wavefunctions to inclusive multi-parton final states in collisions. The key expression eq. (3) is one of the results of this approach. It provided a detailed understanding of the ridge in A+A collisions at RHIC. It predicts a ridge in p+p collisions.

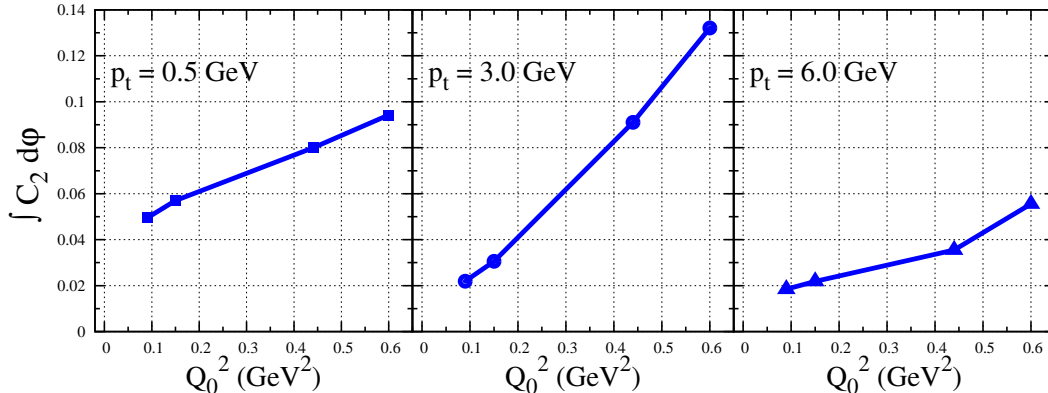


FIG. 6: The correlation function C_2 for different p_\perp as a function of Q_0^2 , the saturation scale at the initial condition of the evolution $x = x_0$. Increasing values of Q_0 correspond to smaller impact parameters and larger total charged multiplicities.

We computed in this paper the two-particle correlation C_2 (eq. (2)) and showed that it shares the same key features as the quantity R measured by the CMS experiment:

- It is long range in rapidity, and exhibits a collimation for high multiplicity events for a narrow window of a few GeV in the transverse momenta of the pair particles. The effect becomes systematically weaker both below and above the kinematic window as seen in the CMS result.
- The two-particle correlation has the same strength for both like and unlike sign pairs. This feature was seen already at RHIC and is consistent with gluon emission from a source that is (nearly) uniform in rapidity, “the glasma flux tube”. It is not consistent with emission from jets.
- The two-particle correlation is relatively flat in the η_1 versus η_2 plane. Again, this feature is natural for gluon emission from nearly boost invariant classical sources. We predict a similarly flat signal strength in three-particle correlations [24].

Correlations of trigger particles at non central rapidities with associated particles at other rapidities can provide sensitive tests of this picture. In order to make a quantitative comparison one needs to add the short range jet component (which can be generated with one of the available

event-generators) to our long range correlation. After including fragmentation one could then form the same quantities as measured in experiment. This is left for further study.

Acknowledgements

We would like to acknowledge James (Bj) Bjorken who in conversations with us at BNL and at the INT in May 2010 was enthusiastic about the prospects of observing the ridge in pp collisions. We gratefully acknowledge useful conversations with Larry McLerran, Robert Pisarski and Nick Samios. We thank Gunther Roland and David Wei Li of the CMS collaboration for communications regarding the experimental findings. A.D. and J.J-M. gratefully acknowledge support by the DOE Office of Nuclear Physics through Grant No. DE-FG02-09ER41620 and from The City University of New York through the PSC-CUNY Research Award Program, grant 63382-00 41. K.D. and R.V. were supported by the US Department of Energy under DOE Contract No. DE-AC02-98CH10886. T.L. is supported by the Academy of Finland, project 126604. F.G. is supported in part by Agence Nationale de la Recherche via the program ANR-06-BLAN-0285-01. T.L. and F.G. thank the Institute for Nuclear Theory at the University of Washington for partial support during the completion of this work.

[1] [CMS Collaboration], arXiv:1009.4122.

[2] J. Adams, *et al.*, [STAR Collaboration] Phys. Rev. Lett. **95**, 152301 (2005).

[3] J. Adams, *et al.*, [STAR Collaboration] Phys. Rev. **C 73**, 064907 (2006).

[4] A. Adare *et al.* [PHENIX Collaboration], Phys. Rev. **C 78**, 014901 (2008).

[5] B. I. Abelev *et al.* [STAR Collaboration], Phys. Rev. **C 80**, 064912 (2009)

[6] B. Alver *et al.* [PHOBOS Collaboration], Phys. Rev.

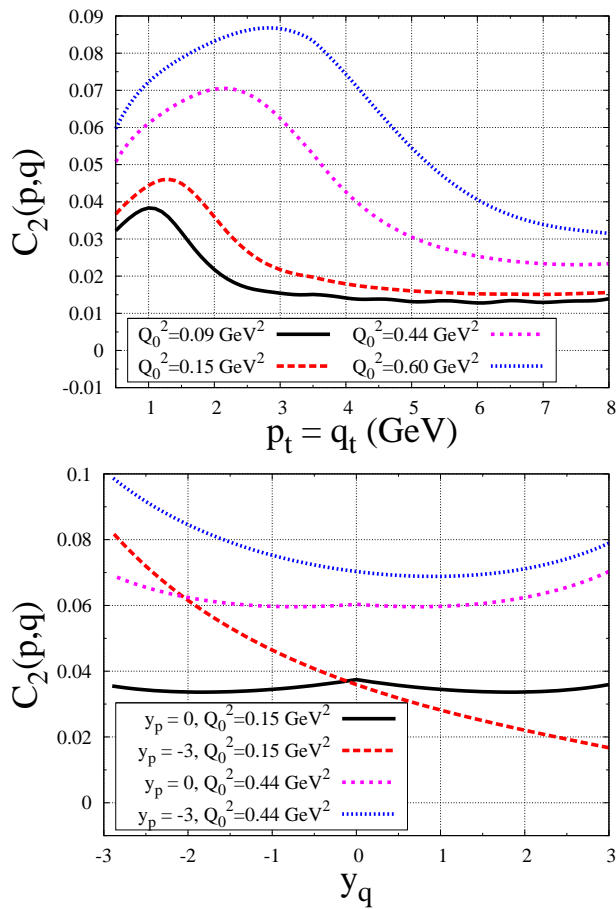


FIG. 7: Top: p_\perp dependence of C_2 at $\Delta\phi \approx 0$ for four different initial scales ranging from minimum bias events to high multiplicity events. Bottom: Rapidity dependence of C_2 at $\Delta\phi = 0$ for $p_\perp = q_\perp = 2$ GeV as a function of y_q , for two different initial scales and y_p . See text for discussion.

Lett. **104**, 062301 (2010).
 [7] B. Alver *et al.* [PHOBOS Collaboration], Phys. Rev. C **81**, 034915 (2010).
 [8] A. Dumitru, F. Gelis, L. McLerran, R. Venugopalan, Nucl. Phys. A **810**, 91 (2008).
 [9] K. Dusling, F. Gelis, T. Lappi, R. Venugopalan, Nucl. Phys. A **836**, 159 (2010).
 [10] A. Dumitru, J. Jalilian-Marian, Phys. Rev. D **81**, 094015 (2010).
 [11] F. Gelis, T. Lappi, R. Venugopalan, Phys. Rev. D **79**, 094017 (2009).
 [12] L.V. Gribov, E.M. Levin, M.G. Ryskin, Phys. Rept. **100**, 1 (1983).
 [13] A.H. Mueller, J-W. Qiu, Nucl. Phys. B **268**, 427 (1986).

[14] E. Iancu, A. Leonidov, L.D. McLerran, Lectures given at Cargese Summer School on QCD Perspectives on Hot and Dense Matter, Cargese, France, 6-18 Aug 2001, hep-ph/0202270.
 [15] E. Iancu, R. Venugopalan, Quark Gluon Plasma 3, Eds. R.C. Hwa and X.N. Wang, World Scientific, hep-ph/0303204.
 [16] F. Gelis, E. Iancu, J. Jalilian-Marian, R. Venugopalan, arXiv:1002.0333.
 [17] A. Kovner, L.D. McLerran, H. Weigert, Phys. Rev. D **52**, 3809 (1995).
 [18] D. Kharzeev, A. Krasnitz, R. Venugopalan, Phys. Lett. B **545**, 298 (2002).
 [19] T. Lappi, L.D. McLerran, Nucl. Phys. A **772**, 200 (2006).
 [20] F. Gelis, T. Lappi, R. Venugopalan, Phys. Rev. D **78**, 054019 (2008).
 [21] F. Gelis, T. Lappi, R. Venugopalan, Phys. Rev. D **78**, 054020 (2008).
 [22] S. Gavin, L. McLerran, G. Moschelli, Phys. Rev. C **79**, 051902 (2009).
 [23] T. Lappi, S. Srednyak, R. Venugopalan, JHEP **1001** 066 (2010).
 [24] K. Dusling, D. Fernandez-Fraile, R. Venugopalan, Nucl. Phys. A **828**, 161 (2009).
 [25] F. Gelis, T. Lappi, L. McLerran, Nucl. Phys. A **828**, 149 (2009).
 [26] S.A. Voloshin, Phys. Lett. B **632**, 490 (2006).
 [27] E.V. Shuryak, Phys. Rev. C **76**, 047901 (2007).
 [28] C.A. Pruneau, S. Gavin, S.A. Voloshin, Nucl. Phys. A **802**, 107 (2008).
 [29] J. Takahashi *et al.*, Phys. Rev. Lett. **103**, 242301 (2009).
 [30] G. Moschelli and S. Gavin, Nucl. Phys. A **836**, 43 (2010).
 [31] K. Werner, I. Karpenko, T. Pierog, M. Bleicher and K. Mikhailov, arXiv:1004.0805 [nucl-th].
 [32] A. Dumitru, in RIKEN-BNL Center Workshop on “Progress in High pT Physics at RHIC”, March 17 – 19, 2010, RBRC Vol. 95, page 129.
 [33] Yu.V. Kovchegov, A.H. Mueller, Nucl. Phys. B **529**, 451 (1998).
 [34] M.A. Braun, Phys. Lett. B **483**, 105 (2000).
 [35] H. Fujii, F. Gelis, R. Venugopalan, Nucl. Phys. A **780**, 146 (2006).
 [36] J.L. Albacete, N. Armesto, J.G. Milhano, C.A. Salgado, Phys. Rev. D **80**, 034031 (2009).
 [37] J. L. Albacete and C. Marquet, Phys. Lett. B **687**, 174 (2010).
 [38] I. Balitsky, Phys. Rev. D **70**, 114030 (2004).
 [39] Yu.V. Kovchegov, Phys. Rev. D **55**, 5445 (1997).
 [40] F. Dominguez, B.W. Xiao, F. Yuan, arXiv:1009.2141.
 [41] H. Kowalski, L. Motyka, G. Watt, Phys. Rev. D **74**, 074016 (2006).
 [42] E. Levin and A. H. Rezaeian, Phys. Rev. D **82**, 054003 (2010).
 [43] J. P. Blaizot, T. Lappi and Y. Mehtar-Tani, Nucl. Phys. A **846**, 63 (2010).